Phase behaviour of syndiotactic polystyrene–*o*-xylene

F. Deberdt and H. Berghmans*
Laboratory for Polymer Research, Katholieke Universiteit Leuven, Celestijnenlaan 200F, B-3001 Leuven, Belgium
(Received 15 March 1993; revised 25 August 1993)

The study of the phase behaviour of syndiotactic polystyrene (sPS) in *o*-xylene is reported. Differential scanning calorimetry, microcalorimetry, infra-red spectroscopy, wide angle X-ray scattering, transmission electron microscopy and thermogravimetric analysis have been used. The polymer chains can adopt a T_2G_2 helix or a planar T_4 zig-zag conformation, depending on the experimental conditions. The initial concentration, the cooling rate and the thermal history strongly influence the formation and the relative contribution of the different conformations, leading to a complex phase behaviour. A decrease of the polymer concentration, and/or an increase of the scanning rate, tends to favour the formation of the helical structure. This helical conformation is always formed when a vitrified, concentrated solution is heated. The transformation of the helical conformation into the planar zig-zag conformation proceeds by a two-step mechanism of melting and recrystallization. Solvent-induced crystallization of amorphous, glassy sPS results in the formation of the helical conformation. The zig-zag conformation is always formed by crystallization from the pure melt. The formation of an incongruent polymer–solvent compound is proposed to explain the complex phase behaviour.

(Keywords: syndiotactic polystyrene; xylene; phase behaviour)

INTRODUCTION

Recent advances in the study of the crystalline structures of highly syndiotactic polystyrene (sPS) have illustrated a very complex polymorphic behaviour[1–16], and four major crystalline phases have been proposed[3–16]. Two crystalline forms, α- and β-phase, containing molecular chains with a zig-zag conformation (T_4), and two crystalline forms, γ- and δ-phase, containing molecular chains with a helical conformation (T_2G_2) have been described. The α- and β-phase have a different chain packing[8,14]. A further distinction has been made between a limiting disordered modification (α' and β') and a limiting ordered modification (α'' and β'')[6,9,15]. Two different structures, in which the molecules adopt a helical conformation, can be obtained from solution or by swelling with a solvent. A completely desiccated sample is called the γ-phase. Drying under milder conditions results in the formation of the δ-phase in which solvent molecules are included. This crystalline phase is presented as a clathrate structure in which the solvent molecule is a guest in the host polymer matrix.

EXPERIMENTAL

The polymer samples were kindly supplied by Idemitsu Kosan Co., Japan, and Dow Chemical Co., MI, USA; they will be referred to as sPS1 and sPS2, respectively. The molecular weight and distribution were determined by gel permeation chromatography in 1,2,4-trichlorobenzene at 125°C. The weight and number average molecular weights are, respectively, 7.9×10^4 and 2.9×10^4 for sPS1 and 18.5×10^4 and 7.2×10^4 for sPS2.

The solvent was obtained from Janssen Chimica and was used without further purification.

The thermal behaviour of the polymer was studied by differential scanning calorimetry (d.s.c.), using a Perkin–Elmer DSC-2C equipped with a thermal analysis data station and a Microcalorimeter Setaram BT200. A cooling and heating rate of $5°\mathrm{C\,min^{-1}}$ was used throughout this work. The use of other scanning rates is specified in the text.

The i.r. spectra were recorded with a Perkin–Elmer 882 i.r. spectrometer. The polymer samples were placed between NaCl windows surrounded by a heating stage. This allowed the polymer solutions to be annealed at various temperatures.

The crystal structure was analysed by wide angle X-ray scattering (WAXS) using CuKα radiation and a Philips PW 1729 flat film camera.

A Stanton Redcroft STA 780 series and a Setaram TGDSC 111 apparatus were used for thermogravimetric analysis (t.g.a.). The samples were heated at $2°\mathrm{C\,min^{-1}}$ under an inert argon or nitrogen atmosphere.

Transmission electron microscopy (TEM) was performed using a Jeol PX 2000 with an acceleration voltage of 200 kV.

The polymer weight fraction (φ_2) is used to express the polymer concentration.

---

* To whom correspondence should be addressed

0032-3861/94/08/1694–11

RESULTS

*Phase behaviour of the system sPS–*o*-xylene*

Dynamic observations of crystallization and melting. The temperature–concentration (T–φ_2) phase diagram of the system sPS–*o*-xylene was investigated by d.s.c. The procedure and its justification have been reported in a previous paper[16]. On cooling the system sPS–*o*-xylene, structure formation results in an exothermic signal. The temperature at the onset of this exotherm is reported as the crystallization temperature, T_c. Its concentration dependence represents the 'crystallization line', whose position on the temperature scale depends on the cooling rate.

Heating results in a melting transition which is reflected by an endothermic signal. The temperature at the end of this endotherm is reported as the melting temperature, T_m.

At high polymer concentrations a glass transition, T_g, is observed. Its position on the temperature scale is important for understanding the phase behaviour.

The calorimetric data are combined with structural information obtained from WAXS observations. The characterization of the different phases has been based on comparison with the most typical lattice spacings reported in the literature; these are reported in *Table 1*.

It is impossible to differentiate between the α- and β-phase by flat film recording. Therefore, the zig-zag structure will be referred to as the β-phase because this crystalline modification, described in the literature, has been formed in the presence of solvent. The crystallization temperatures of the δ-phase and the β-phase will be referred to as T_c^δ and T_c^β, while the melting temperatures of these phases will be called T_m^δ and T_m^β, respectively. The crystallization enthalpy of the δ-phase and the β-phase will be referred to as ΔH_c^δ and ΔH_c^β, while the melting enthalpy of these phases will be called ΔH_m^δ and ΔH_m^β, respectively.

*The system sPS1–*o*-xylene.* The temperature–concentration phase diagrams of sPS1–*o*-xylene are represented in *Figure 1*. Three concentration regions are considered.

(i) Low concentration region ($\varphi_2 < 0.50$). Cooling of a moderately concentrated solution results in the formation of an elastic, opaque gel. Only one exotherm is observed in the corresponding d.s.c. experiment (*Figure 2A*). WAXS observations reveal the formation of the δ-phase in which the polymer chain adopts a helical conformation. Heating results in a single endotherm (*Figure 2B*). Both T_c^δ and T_m^δ increase with increasing polymer concentration.

(ii) Intermediate concentration region ($0.50 < \varphi_2 < 0.75$).

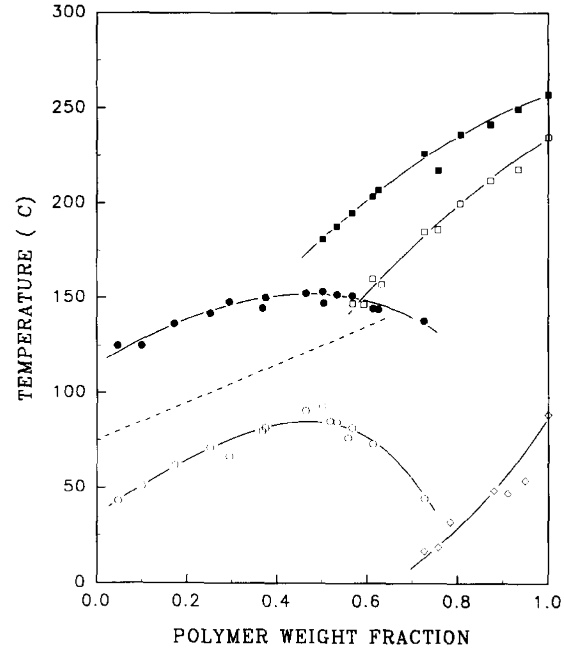

Figure 1 Phase diagram of sPS1 in *o*-xylene: ○, crystallization of δ-phase; □, crystallization of β-phase; ●, melting of δ-phase; ■, melting of β-phase; ◇, glass transition; ---, temperature limit of the coil-to-helix transition

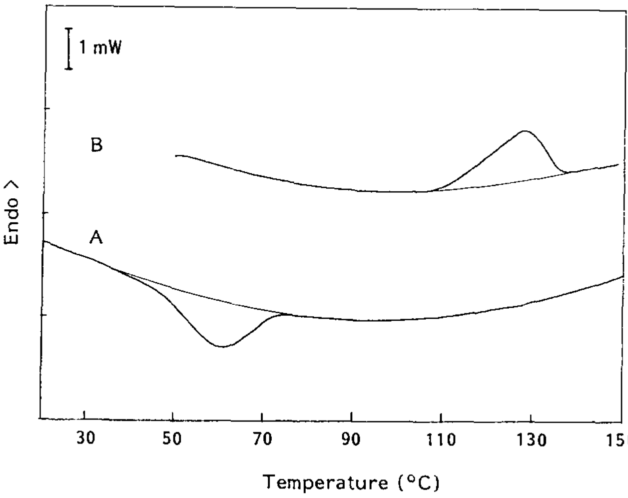

Figure 2 D.s.c. thermograms of sPS2–*o*-xylene ($\varphi_2 = 0.15$): A, cooling; B, heating

Table 1 Comparison between the experimentally observed WAXS data and those reported in the literature[6]: A, crystallization from a homogeneous solution ($\varphi_2 = 0.10$), cooled at 5°C min^{-1}, that has been dried under reduced pressure at room temperature: formation of the δ-phase; B, diffraction results for the δ-phase obtained by Guerra *et al.*[6]; C, crystallization from a homogeneous solution ($\varphi_2 = 0.90$), cooled at 5°C min^{-1}: formation of the β-phase; D, diffraction results for the β-phase obtained by Guerra *et al.*[6] [a]

A		B		C		D	
Lattice spacing (Å)	Intensity[b]	Lattice spacing (Å)	Intensity[b]	Lattice spacing (Å)	Intensity[b]	Lattice spacing (Å)	Intensity[b]
11.3	s	11.32	m	14.1	m	14.34	ms
5.2	s	5.21	vs	6.5	s	6.49	m
3.8	s	3.88	s	4.8	m	4.78	m
3.2	m	3.10	w	2.1	vw		

[a] In ref. 16, Table 1, these data have also been presented but β was wrongly used instead of δ and vice versa

[b] vs, very strong; s, strong; ms, medium/strong; m, medium; w, weak; vw, very weak

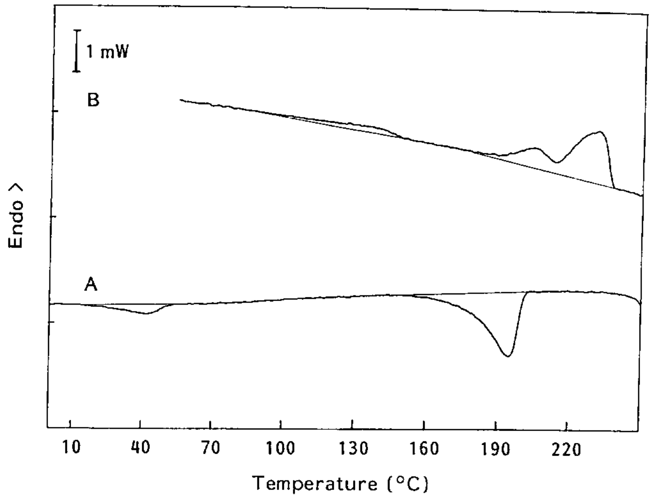

Figure 3 D.s.c. thermograms of sPS2–*o*-xylene ($\varphi_2 = 0.63$): A, cooling; B, heating

Two exotherms are observed upon cooling (*Figure 3A*), while heating results in three endotherms (*Figure 3B*). The low temperature exotherm corresponds to the formation of the δ-phase. The corresponding T_c^δ decreases with increasing polymer concentration. The melting of the δ-phase results in a single melting endotherm at low temperature. Its melting temperature decreases slightly with increasing polymer concentration. The exotherm at high temperature is ascribed to the formation of the β-phase. The corresponding melting signal is composed of two partially overlapping endotherms. This is ascribed to a dynamic recrystallization during heating. Confirmation of this recrystallization is obtained from heating experiments performed at different scanning rates. The contribution of the high temperature part of this endotherm decreases with increasing heating rate.

An important difference between the concentration dependence of T_m^β and T_m^δ is observed. An increase in the polymer concentration results in an increase of T_m^β and the surface of the corresponding melting endotherm, and in a decrease of T_m^δ and the surface of the corresponding melting endotherm.

(iii) High concentration region ($\varphi_2 > 0.75$). Only one exotherm is observed when highly concentrated solutions are cooled. Heating results in a double melting endotherm. These transitions correspond to the formation and the melting of the β-phase. This has been verified with WAXS measurements (*Table 1*). Both T_c^β and T_m^β increase with increasing polymer concentration. The double signal registered upon heating is also ascribed to a dynamic recrystallization during the melting of the β-phase.

Influence of the molecular weight. The phase diagram for the system sPS2–*o*-xylene is represented in *Figure 4*. An increase of the molecular weight results in a higher value for T_m^β and T_c^β of the solvent-free polymer and the solutions. It does not influence the formation and the melting of the δ-phase.

Melting enthalpy. The melting endotherms of the β- and the δ-phase have been integrated separately. The corresponding melting enthalpies are corrected for the presence of solvent and these reduced values are plotted as a function of polymer concentration in *Figure 5*.

The melting enthalpy of the δ-phase is high in the dilute concentration region, approaches a plateau value around 30 J g^{-1} for $0.15 < \varphi_2 < 0.35$, and finally decreases over a narrow concentration range at higher concentrations. The melting enthalpy of the β-phase is zero in the low concentration region but reaches a high value of $\Delta H_m^\beta = 30$ J g^{-1} around $\varphi_2 = 0.50$ and decreases slightly towards higher polymer concentrations.

Influence of the cooling rate. (i) Low concentration region. The formation of the δ-phase on cooling has also been followed with the more sensitive Setaram BT200 microcalorimeter. A more complex signal is obtained than

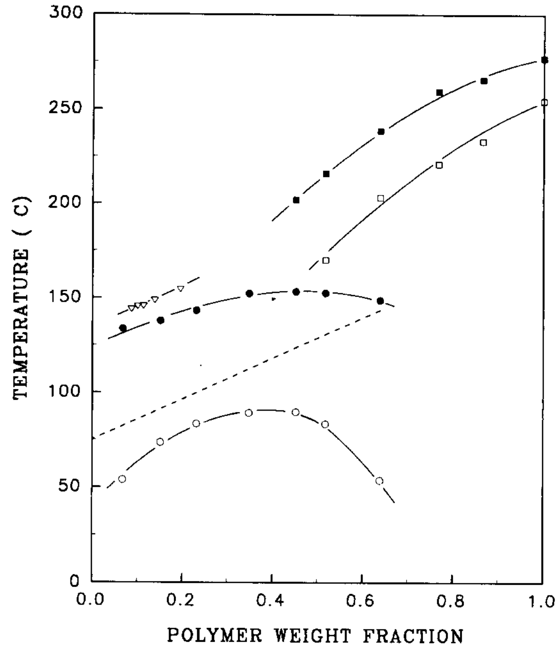

Figure 4 Phase diagram of sPS2 in *o*-xylene: ○, crystallization of δ-phase; □, crystallization of β-phase; ●, melting of δ-phase; ■, melting of δ-phase; ▽, melting of β-phase after isothermal crystallization at 110°C; ---, temperature limit of the coil-to-helix transition

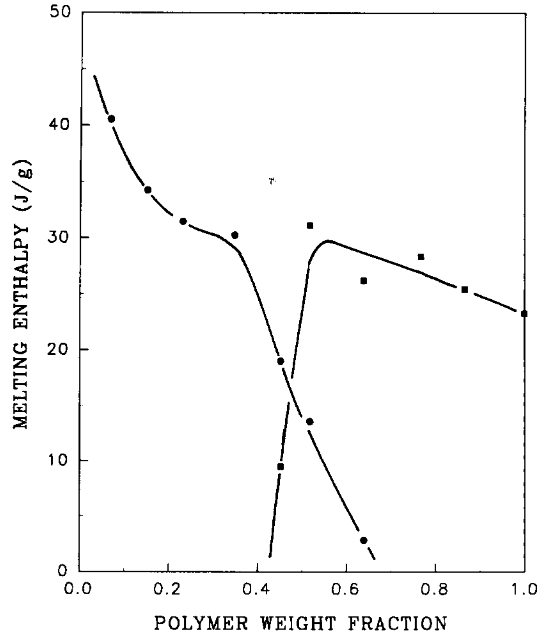

Figure 5 Influence of polymer concentration on melting enthalpy of sPS2: ●, melting enthalpy of δ-phase; ■, melting enthalpy of β-phase

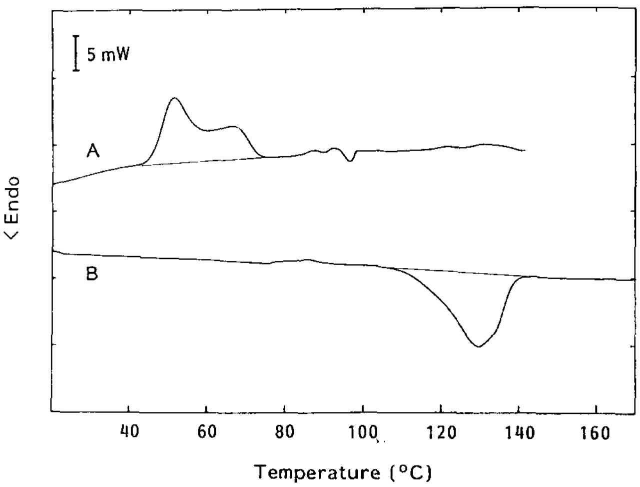

Figure 6 Microcalorimetric thermogram of sPS2–*o*-xylene ($\varphi_2 = 0.15$), scanning rate = 0.5°C min^{-1}: A, cooling; B, heating

that recorded with d.s.c. A typical scan is represented in *Figure 6* for a dilute solution cooled and heated at 0.5°C min^{-1}. The temperature at the onset of the exothermic signal is similar to the onset temperature obtained with d.s.c. measurements, but the signal is composed of two exothermic signals. The endotherm registered in the subsequent melting experiment consists of only one peak. The temperature at the end of this endotherm corresponds to the melting point of the δ-phase obtained by d.s.c. A decrease of the cooling rate narrows the exothermic signal owing to a shift to higher temperatures of the low temperature part of this complex signal. The melting and crystallization enthalpies are similar to the values obtained from d.s.c. measurements. The results, summarized in *Table 2*, reveal a small increase in both ΔH_c^δ and ΔH_m^δ with decreasing cooling rate.

(ii) Intermediate concentration region. The influence of the cooling rate on the melting and crystallization behaviour has been investigated in the intermediate concentration region where both phases are formed. The data from d.s.c. measurements are reported in *Table 3*.

An important decrease of the crystallization temperature of the β-phase and the corresponding crystallization enthalpy is observed when the scanning rate is increased. The crystallization temperature of the δ-phase, on the other hand, is only slightly affected by a change of the cooling rate, while the corresponding crystallization enthalpy increases with increasing cooling rate. The opposite rate dependence of the crystallization enthalpy of the δ- and the β-phase is clearly reflected in the cooling rate dependence of their ratio, $\Delta H_c^\beta/\Delta H_c^\delta$.

A good insight into the influence of the cooling rate on the melting behaviour and into the relative contribution of both phases is obtained from heating experiments performed with samples cooled at different scanning rates but heated in the d.s.c. at 5°C min^{-1}. The data are reported in *Table 4*. A small increase of T_m^β is recorded while T_m^δ remains constant.

Comparison between the crystallization and melting enthalpies clearly illustrates the recrystallization from the δ- into the β-phase. The difference between ΔH_m^β and ΔH_c^β increases with increasing cooling rate owing to an increased reduction of the extent of crystallization of the β-phase at higher scanning rates. The almost constant value of ΔH_m^β results from recrystallization of part of the δ-phase into the β-phase.

Formation of the β-phase in the low concentration region

The β-phase cannot be formed in the low concentration region during a dynamic experiment. It is, however, possible to form this phase at these low concentrations by isothermal annealing of solutions at high temperature.

When a dilute solution of sPS2 and *o*-xylene ($\varphi_2 = 0.005$) is annealed at temperatures above 70°C for a period of several weeks, crystals are formed. The WAXS pattern reveals the formation of the β-phase. Annealing at 70°C or lower results in the formation of the δ-phase.

Dilute solutions of sPS1 and *o*-xylene do not crystallize after annealing at high temperature. The highest temperature at which structure formation can be observed by isothermal annealing is 90°C. At this temperature, however, the polymer chains adopt the helicoidal conformation extremely slowly and this results in the formation of the δ-phase.

The melting behaviour of crystals prepared at high temperature from a very dilute solution was studied. These crystals (β-phase) were suspended in *o*-xylene and their melting behaviour studied optically. The temperature at which the solution becomes completely transparent is recorded as the final melting point. The melting point is plotted in *Figure 7* as a function of the weight fraction of polymer in the suspension.

Annealing of more concentrated solutions of sPS2 at high temperature results in the formation of a transparent gel, which slowly turns turbid on prolonged annealing. The temperature at which the opalescence disappears is close to the melting point of the δ-phase obtained from d.s.c. measurements. This melting point, however, is much lower than the melting point obtained with the crystal suspensions.

Table 2 Melting and crystallization enthalpies of a solution of sPS2–*o*-xylene ($\varphi_2 = 0.15$) obtained by d.s.c. and microcalorimetry (Calvet)

Technique (scanning rate, °C min^{-1})	ΔH_c (J g^{-1})	ΔH_m (J g^{-1})
D.s.c. (−/+5)	−34.5	34.3
Calvet (−/+0.5)	−38.9	42.9
Calvet (−/+0.2)	−41.8	43.9

Table 3 Influence of cooling rate on the crystallization behaviour of a solution of sPS1–*o*-xylene, $\varphi_2 = 0.54$

Cooling rate (°C min^{-1})	T_c^δ (°C)	ΔH_c^δ (J g^{-1})	T_c^β (°C)	ΔH_c^β (J g^{-1})	$\Delta H_c^\beta/\Delta H_c^\delta$
5	82.6	−8.7	137.7	−9.6	1.1
10	83.7	−13.3	134.9	−8.1	0.6
20	83.1	−17.8	126.6	−4.4	0.3
40	78.6	−31.7	116.6	−1.7	0.1

Table 4 Influence of cooling rate on the melting behaviour of a solution of sPS1–*o*-xylene, $\varphi_2 = 0.54$ (heating rate 5°C min^{-1})

Cooling rate (°C min^{-1})	T_m^δ (°C)	ΔH_m^δ (J g^{-1})	T_m^β (°C)	ΔH_m^β (J g^{-1})	$\Delta H_m^\beta/\Delta H_m^\delta$
5	154.4	8.1	186.1	11.9	1.5
10	154.5	17.6	188.1	13.0	0.7
20	153.1	23.2	190.0	12.8	0.6
40	154.3	31.7	192.0	11.5	0.4

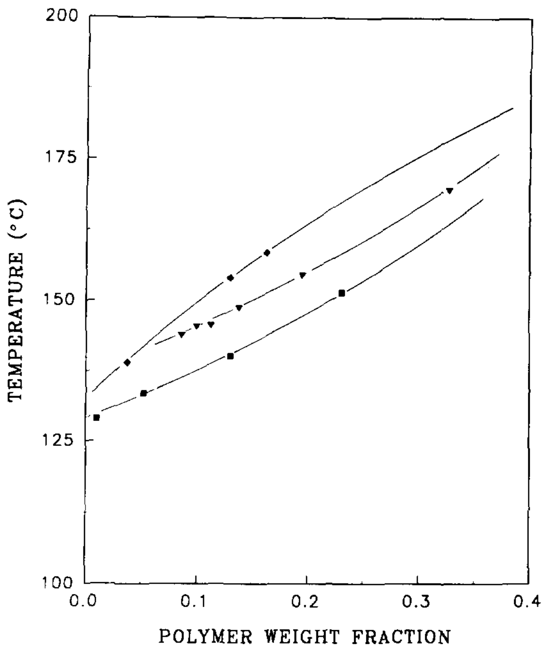

Figure 7 Melting of the β-phase, crystallized under different experimental conditions (sPS2): ■, isothermal crystallization at 110°C, optical observation; ▼, isothermal crystallization at 110°C, d.s.c. measurement; ◆, suspensions of zig-zag conformation, optical observation

A turbid gel, formed from a dilute solution which was crystallized at 110°C, was partially dried at room temperature and heated in the d.s.c. The melting point of samples taken after different drying times was measured. A broad and irregular endothermic signal is always obtained and the corresponding melting temperature is situated between the optical measured melting temperature of the turbid gel and of the suspensions. These results are also summarized in *Figure 7*.

Formation and thermal behaviour of the δ-phase

The formation of the δ-phase during a cooling experiment at moderate scanning rates in the intermediate and high concentration region is difficult. The polymer crystallizes almost completely into the β-phase. The formation of the δ-phase in this domain, however, is not excluded, and three different roads can be followed: quenching, drying or swelling. The samples have been subjected to three successive d.s.c. experiments: heating (first scan), cooling and a second heating (second scan).

Quenching of solutions. (i) Melting of quenched solutions. The thermal behaviour of moderately and highly concentrated solutions quenched in liquid nitrogen depends strongly on the initial concentration and on the scanning rate at which the melting is performed. The homogeneous solutions, quenched in liquid nitrogen, are transferred at this low temperature into the d.s.c. cell.

The d.s.c. thermogram of highly concentrated quenched solutions ($\varphi_2 > 0.80$) first shows a glass transition, followed at higher temperature by a crystallization exotherm, a second exothermic signal and an endotherm (*Figure 8A*). This can be explained as follows. An amorphous, glassy sample is obtained on quenching. Heating above its glass transition temperature (T_g) results in crystallization with the formation of the δ-phase. WAXS analysis, carried out on samples annealed at around 120°C, proves that the polymer chains have adopted the δ-phase helical conformation. The second exothermic signal, at around 155°C, is caused by the transition of the δ-phase to the more stable β-phase. This transition is confirmed by WAXS data obtained with samples annealed at 190°C. Finally, at high temperature the broad melting endotherm of the β-phase is registered. No dynamic recrystallization is observed and the final melting temperature corresponds to that observed for the β-phase in dynamic experiments.

There is no indication of the melting of the δ-phase. This absence of the melting endotherm of the δ-phase and the important difference in size between the formation exotherm and the melting endotherm of the β-phase is ascribed to the typical formation mechanism of the β-phase under these conditions[16]. The δ-phase melts upon heating and recrystallizes into the β-phase. Both phenomena take place almost simultaneously and only a small differential exothermic signal is registered as a result of the overlapping of the melting endotherm of the δ-phase and the recrystallization exotherm of the β-phase.

This mechanism is confirmed by d.s.c. measurements performed with annealed samples, heated at different scanning rates. The samples are submitted to a specific thermal treatment to exclude differences in thermal history. The solution with $\varphi_2 = 0.90$ is quenched in liquid nitrogen and the glassy sample obtained is heated at 5°C min^{-1} up to 130°C. This temperature is situated between the exotherm ascribed to the formation of the δ-phase and the exotherm representing the transition of the δ-phase to the β-phase. This annealed sample was subjected to heating scans at 5 and at 40°C min^{-1}.

The d.s.c. thermogram recorded at 5°C min^{-1} shows only an exotherm ($\Delta H = -4.4\,J\,g^{-1}$) caused by the transition to the β-phase and an endotherm corresponding to the melting of the β-phase. It is similar to the thermogram represented in *Figure 8A*.

When the sample is heated at 40°C min^{-1}, a small endotherm ($\Delta H = 1.5\,J\,g^{-1}$) is registered, caused by the (partial) melting of the δ-phase. The temperature at the end of this endotherm is about 150°C (*Figure 9*). This melting signal is immediately followed by an exotherm ($\Delta H = -6.6\,J\,g^{-1}$) and, at higher temperature, by an

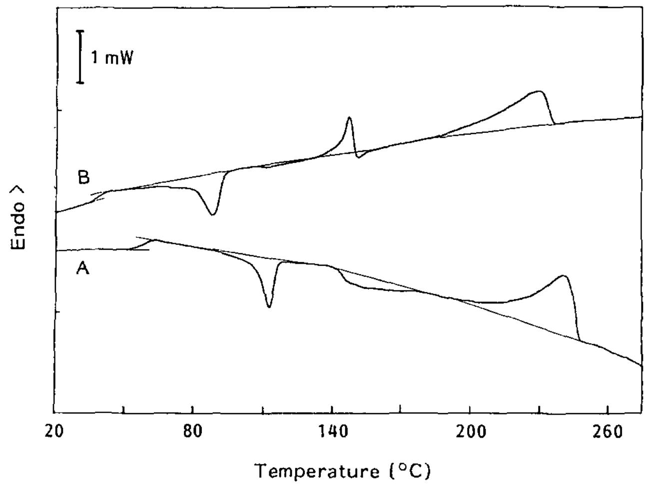

Figure 8 D.s.c. thermogram of solutions of sPS1–o-xylene, quenched in liquid nitrogen: A, $\varphi_2 = 0.91$; B, $\varphi_2 = 0.78$

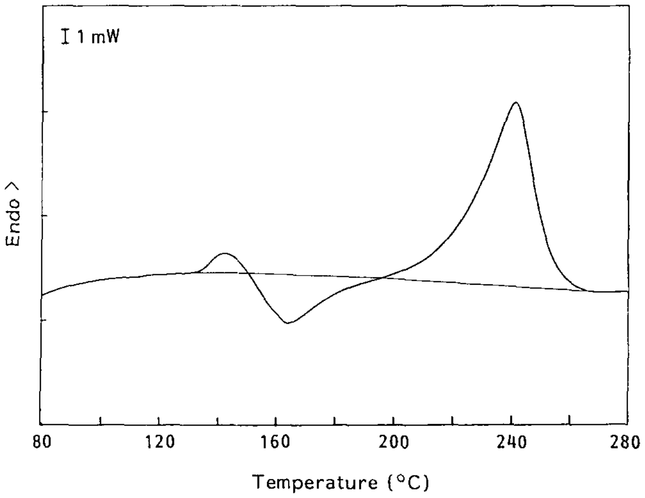

Figure 9 D.s.c. thermogram of a solution of sPS1–*o*-xylene, quenched in liquid nitrogen, $\varphi_2=0.90$, heated at 5°C min^{-1} to 130°C, cooled to room temperature, and heated at 40°C min^{-1}

Table 5 Influence of scanning rate on crystallization and melting behaviour of a quenched solution of sPS1–*o*-xylene ($\varphi_2=0.88$)

	Scanning rate (°C min^{-1})			
	5	10	20	40
T_g (°C)	48.5	51.0	60.0	69.0
$T_c^{\mathrm{min}\delta}$ (°C)	109.3	119.5	131.4	177.1
$T_{tr}^{\mathrm{end}\delta}$ (°C)	202.9	198.2	204.7	210.1
$T_m^{\mathrm{end}\beta}$ (°C)	250.3	253.3	259.4	272.4
ΔH_c^δ (J g^{-1})	−10.0	−12.5	−11.8	−11.2
ΔH_{tr}^β (J g^{-1})	−7.7	−8.0	−6.7	−1.3
ΔH_m^β (J g^{-1})	24.0	26.7	25.6	26.7

endotherm. These two transitions correspond to the recrystallization and the melting of the β-phase.

The scanning rate strongly influences the temperature of the thermal transitions (*Table 5*). The T_g of the quenched sample increases with higher scanning rate. This shift is accompanied by an even greater increase of the crystallization temperature of the δ-phase. The surface corresponding to this exotherm is not affected by the scanning rate. The exotherm corresponding to the recrystallization and resulting in the formation of the β-phase is situated around 190–205°C. This transition temperature is almost independent of the heating rate. The corresponding enthalpy change decreases as the scanning rate increases, while the melting enthalpy of the β-phase remains constant. A small increase in the melting temperature is observed. No melting of the δ-phase is registered even upon heating at 40°C min^{-1}.

The simultaneous melting of the δ-phase and its recrystallization into the β-phase is lost for samples with a lower polymer concentration (*Figure 8B*). An additional endothermic signal, corresponding to the melting of the δ-phase, is followed by the recrystallization exotherm of the β-phase. This partial separation between melting and recrystallization is ascribed to the increase in solvent content.

(ii) Melting of quenched and annealed solutions. Samples annealed in the broad exothermic signal that represents the recrystallization exotherm were analysed by d.s.c. The corresponding d.s.c. scans are presented in *Figure 10* and are compared with the d.s.c. scan obtained without annealing (*Figure 10A*). Annealing at 110°C resulted in a limited decrease in the melting enthalpy of the δ-phase and an important increase of the melting enthalpy of the β-phase (*Figure 10B*). The X-ray diffraction pattern obtained with this sample reveals the presence of the δ-phase and the β-phase. The d.s.c. thermogram of a sample annealed at 152°C (the temperature at the end of the melting signal of the δ-phase) shows only one broad melting endotherm of the β-phase (*Figure 10C*). This annealing procedure leads to a complete transformation into the β-phase.

(iii) Influence of scanning rate. An increase of the scanning rate results in an increase of T_g and of the temperature at the minimum of the crystallization exotherm of the δ-phase ($T_c^{\mathrm{min}\delta}$). The temperature at the end of the recrystallization exotherm ($T_c^{\mathrm{end}\delta}$) and the final melting point of the β-phase ($T_m^{\mathrm{end}\beta}$) are almost unaltered by a change in the scanning rate. The increase in scanning rate has a pronounced influence on the crystallization and melting enthalpy of the δ-phase but has almost no effect on the enthalpy changes of the β-phase. The data are reported in *Table 6*.

(iv) Influence of concentration. The concentration dependence of the T_m^β of these quenched samples is similar to that observed in dynamic experiments. No dynamic recrystallization of the β-phase is observed on heating. The melting point of the δ-phase is independent of the concentration and is located above the values obtained

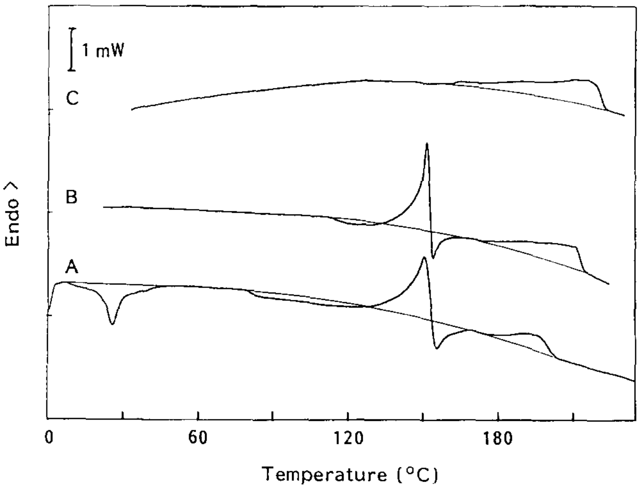

Figure 10 D.s.c. thermograms of solutions of sPS1–*o*-xylene, quenched in liquid nitrogen ($\varphi_2=0.63$): A, without further annealing; B, after annealing at 110°C; C, after annealing at 152°C

Table 6 Influence of scanning rate on crystallization and melting behaviour of a quenched solution of sPS1–*o*-xylene ($\varphi_2=0.75$)

	Scanning rate (°C min^{-1})		
	5	10	20
T_g (°C)	19.0	29.0	38.0
$T_c^{\mathrm{min}\delta}$ (°C)	73.7	99.1	109.2
$T_m^{\mathrm{end}\delta}$ (°C)	147.6	148.9	151.5
$T_c^{\mathrm{end}\beta}$ (°C)	160.1	160.1	169.9
$T_m^{\mathrm{end}\beta}$ (°C)	236.5	239.9	243.5
ΔH_c^δ (J g^{-1})	−17.0	−12.4	−11.3
ΔH_m^δ (J g^{-1})	7.4	2.4	1.6
ΔH_c^β (J g^{-1})	−2.5	−1.0	−1.4
ΔH_m^β (J g^{-1})	31.5	27.7	24.9

in dynamic experiments. These melting data are reported in *Figure 11*.

The decrease of the crystallization and melting enthalpy of the δ-phase and the increase of the melting enthalpy of the β-phase with increasing polymer concentration confirm the data obtained in the dynamic experiments (*Table 7*).

The thermal crystallization of the glassy, amorphous sPS, obtained by quenching from the pure melt, results in the formation of the β-phase. The T_g is located at 90°C and crystallization sets in at 140°C. The melting endotherm is situated at around 270°C and no recrystallization is observed on heating.

Drying of moderately concentrated solutions. (i) Sample preparation. The δ-phase can also be formed in a sample with high polymer concentration by drying a relatively dilute, crystallized solution. In these systems, the polymer adopts the helical conformation. The touch-dry sample obtained still contains 13–15% solvent (*Table 8*). This large amount of solvent cannot be removed by prolonged drying at ambient temperature, but only by heating at 190°C. The initial polymer concentration has almost no influence on the amount of *o*-xylene that is left in these touch-dry samples. When an atactic sample is subjected to the same treatment, only 4% of solvent is left.

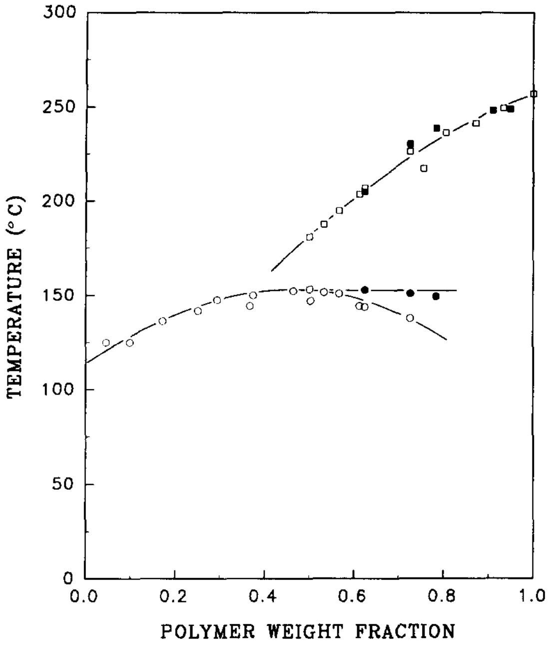

Figure 11 Phase diagram of sPS1 in *o*-xylene: ○, melting of δ-phase, dynamic experiments; □, melting of β-phase, dynamic experiments; ●, melting of δ-phase, after quenching; ■, melting of β-phase, after quenching

Table 7 Influence of concentration of a quenched solution on the crystallization and melting enthalpies

Concentration φ_2	ΔH_c^δ (J g^{-1})	ΔH_m^δ (J g^{-1})	ΔH_m^α (J g^{-1})
0.63	−16.5	22.6	10.0
0.72	−12.2	16.0	24.1
0.78	−14.8	6.9	26.8
0.91	−8.1	–	30.9
0.95	−9.0	–	29.1

(ii) Thermal analysis. The calorimetric analysis of these touch-dry samples of sPS reveals, in the first scan, a small endotherm, followed at higher temperature by a broad exotherm and a sharp, single endotherm (*Figure 12A*). The small endothermic peak (8 J g^{-1}) around 150°C is ascribed to the onset of melting of the δ-phase. The existence of this phase in the low temperature region was confirmed by WAXS. The very broad exothermic signal between 150 and 240°C is ascribed to the transition of the δ-phase to the β-phase. This transition is confirmed by WAXS. At still higher temperature, the melting of the β-phase takes place around 265°C and the corresponding melting enthalpy is 21 J g^{-1}. This is almost 15°C below the melting temperature of melt crystallized sPS and is caused by the presence of a substantial amount of *o*-xylene trapped in the touch-dry sample. A single endothermic signal is recorded. In a second heating scan, after cooling to room temperature, only the melting of the β-phase is registered (*Figure 12B*). A double melting endotherm, characteristic of recrystallization of the β-phase during heating, is observed. The final melting temperature of the β-phase is the same in the first or second scan. The δ-phase is not re-formed on cooling.

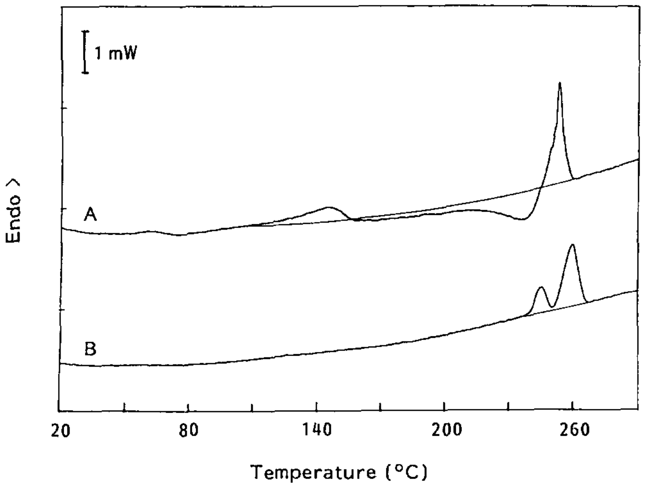

Figure 12 D.s.c. thermograms of a touch-dry δ-phase of sPS2–*o*-xylene: A, first heating scan; B, second heating scan

Table 8 Thermogravimetric results of dried gels of sPS and dried solutions of aPS

System	Initial concentration (%)	*o*-Xylene remaining (%)	Temperature region (°C)	Molar ratio solvent:monomer
sPS–*o*-xylene	10.3	13.7	65–170	1:6.5
sPS–*o*-xylene	5.7	15.4	65–190	1:5.6
aPS–*o*-xylene	5.9	4.0	80–195	

Table 9 WAXS results of a dried gel of sPS–*o*-xylene after annealing at various temperatures

As-cast		Annealed (140°C)		Annealed (190°C)		Melted (280°C) Crystallized (225°C)	
Lattice spacing (Å)	Intensity[a]	Lattice spacing (Å)	Intensity[a]	Lattice spacing (Å)	Intensity[a]	Lattice spacing (Å)	Intensity[a]
11.3	s	9.4	s	14.1	m	14.1	m
5.2	vs	5.5	s	6.5	s	6.5	m
3.8	s	4.4	vs	4.8	m	4.8	m
3.2	m			2.1	vw	2.2	vw

[a] vs, very small; s, small; m, medium; vw, very wide

(iii) X-ray analysis. The conformational changes occurring in a touch-dry gel can be followed with WAXS and i.r. measurements.

Annealing a touch-dry polymer film at 140°C for 15 min results in a slightly different diffraction pattern. This pattern is ascribed to the γ-phase. This is a similar helical structure to the δ-phase but without solvent incorporated in the matrix. T.g.a. reveals that the touch-dry gel has lost most of its solvent at this temperature. A conformational change of the polymer chains takes place when this film is annealed at 190°C. The X-ray diffraction pattern is now characteristic of the β-phase zig-zag conformation. A similar result is obtained for a dried gel melted at 280°C and recrystallized at 225°C. The WAXS results of this annealing experiment are summarized in *Table 9*.

(iv) I.r. analysis. A translucent touch-dry polymer film can be cast from a dilute solution by drying under reduced pressure. I.r. transmission spectroscopy is well suited to the study of conformational changes occurring during annealing at different temperatures (*Figure 13*). A doublet at 943 and 934 cm^{-1} is observed in the spectrum of a cast film. Its intensity changes after annealing at 140°C. The doublet disappears almost completely when the samples are annealed above 190°C, while a signal at 1222 cm^{-1}, absent in the cast film, appears as a sharp band in the spectrum. The relation between the spectroscopic results and the polymer conformation has been described extensively in the literature[7,17–23]. The signal at 1120 cm^{-1}, characteristic of the presence of *o*-xylene, disappears on annealing at 140°C owing to evaporation of the solvent.

(v) Formation of the γ-phase. The d.s.c. trace of the γ-phase, obtained after annealing a touch-dry δ-phase film at 140°C, is very similar to the thermogram of the δ-phase (*Figure 14*). A very small endothermic signal (0.8 $\mathrm{J\,g}^{-1}$) around 190°C is followed by a broad exothermic signal extending from 195 to 265°C. This sequence of signals is ascribed to the transition from the γ-phase to the β-phase which melts at around 280°C. It corresponds to the melting point of the pure polymer. No recrystallization of this β-phase is observed.

Swelling of a glassy phase. An amorphous glassy polymer film is obtained by quenching the sample from the molten state into liquid nitrogen. The amorphous sample is then oriented by stretching the transparent film in boiling water. No crystallization of the sample into the β-phase takes place under these conditions as crystallization is extremely slow at temperatures so close to T_g. The oriented, amorphous film, still fixed in the clamps of the stretcher, is then immersed in *o*-xylene at room temperature. Crystallization into the δ-phase takes place and the original molecular orientation is maintained in the crystallized sample. The formation of the δ-phase is also confirmed by the presence of an absorption peak in the i.r. spectrum at 935 cm^{-1}. A touch-dry sample is obtained with $\varphi_2 = 0.85$. The amount of absorbed solvent in this sample corresponds to what is left when a solution with an initial concentration of $\varphi_2 = 0.10$ is dried at room temperature under vacuum.

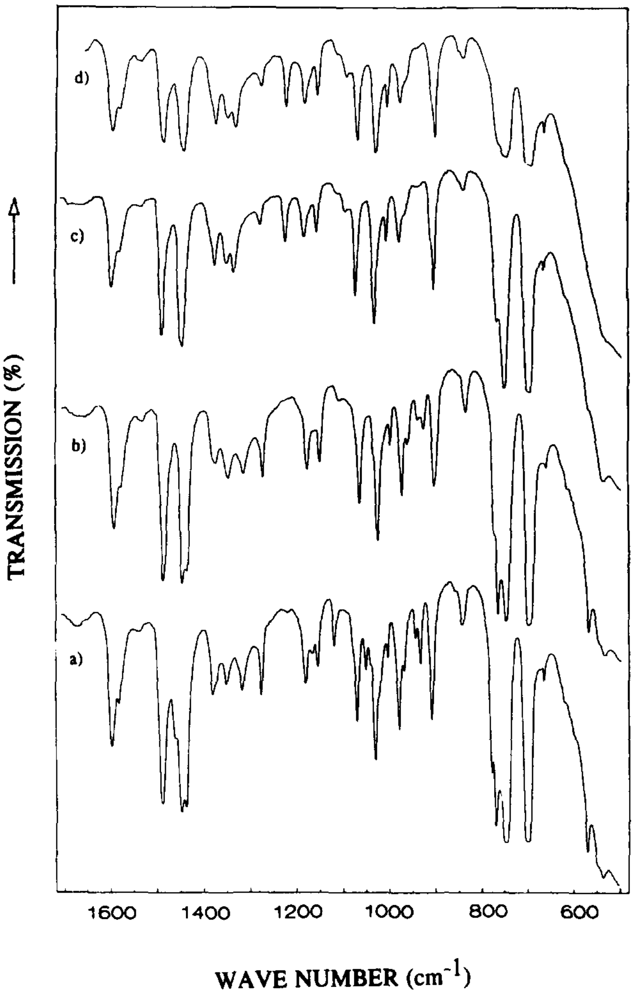

Figure 13 I.r. spectra of a touch-dry δ-phase helical structure of sPS–*o*-xylene: (a) without further annealing; (b) after annealing at 140°C; (c) after annealing at 190°C; (d) after melting at 280°C and crystallization at 225°C

Different transitions take place when the sample is heated in t.g.a.–d.s.c. equipment (*Figure 15*). The solvent evaporates and the δ-phase transforms into the γ-phase. This is reflected in a broad endothermic signal. This

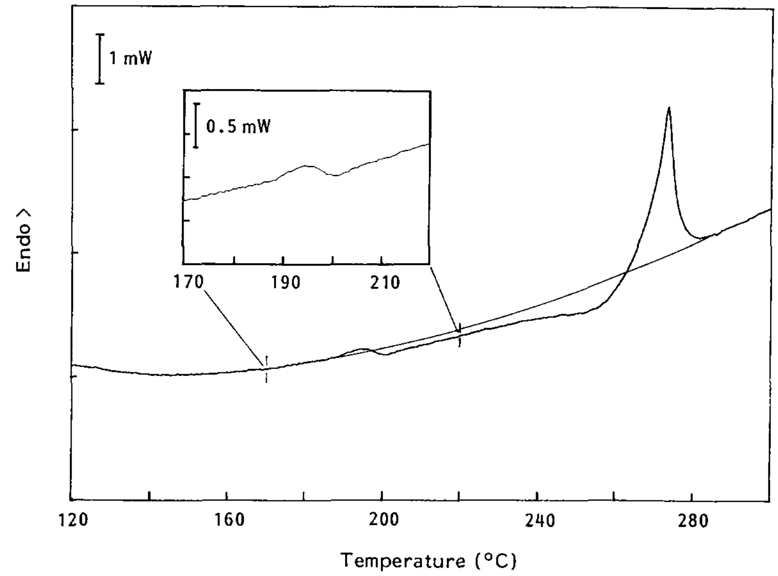

Figure 14 D.s.c. thermogram of a γ-phase of sPS

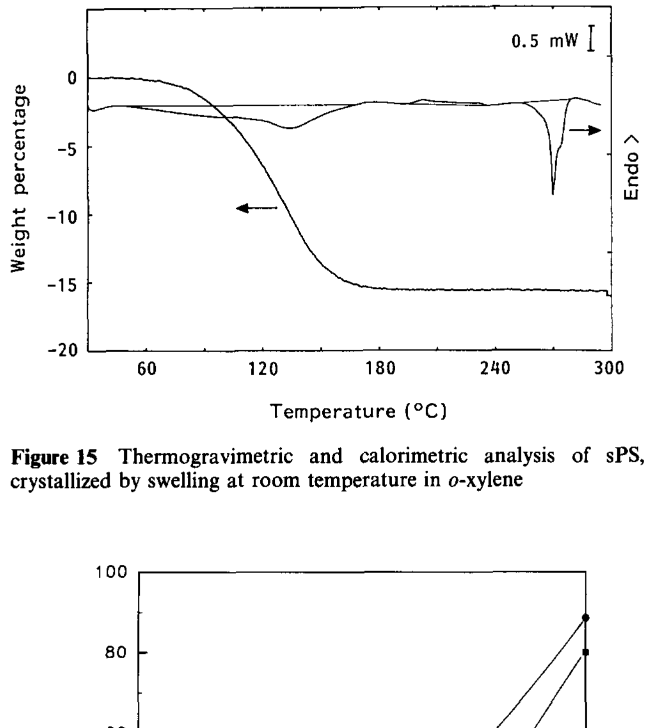

Figure 15 Thermogravimetric and calorimetric analysis of sPS, crystallized by swelling at room temperature in *o*-xylene

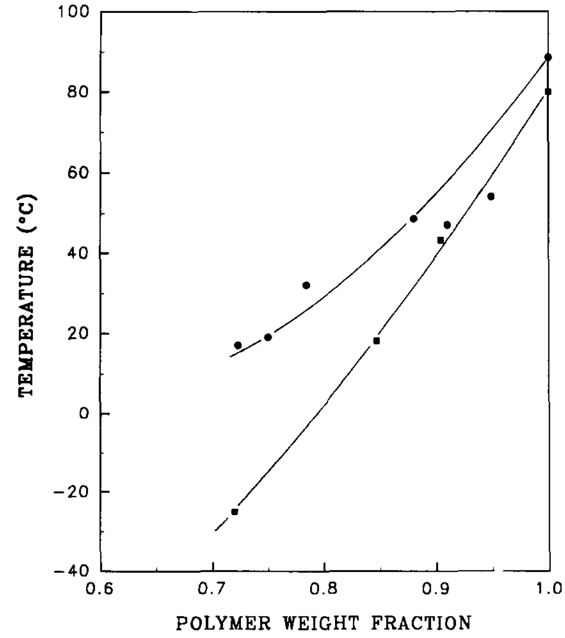

Figure 16 T_g–φ_2 relationship of the system PS–*o*-xylene: ●, syndiotactic; ■, atactic

γ-phase then recrystallizes into the β-phase at around 190°C. The small exothermic signal observed is attributed to the overlapping of melting and recrystallization.

Swelling of the β-phase. A film crystallized from the melt into the β-phase is immersed in *o*-xylene at room temperature. No recrystallization into the δ-phase takes place, even after a period of 50 days. When the sample is immersed in a better solvent, such as chloroform, the transition from the β-phase to the δ-phase proceeds in less than 4 days.

Glass transition. The influence of the solvent content on T_g of the polymer–solvent systems was investigated. Amorphous samples were obtained by quenching the solutions in liquid nitrogen. The T_g–φ_2 relationship is represented in *Figure 16*, together with the relationship obtained with the atactic isomer. A less pronounced decrease of T_g with increasing solvent content is observed for the syndiotactic isomer. The T_g–φ_2 relationship of sPS–*o*-xylene is also reported in *Figure 1*.

DISCUSSION

The complex phase behaviour of sPS in *o*-xylene has many aspects in common with the system sPS–decalin, reported in a previous paper[16]. Three different phases have also been characterized. Their formation and relative contribution to the structure formation is controlled by the experimental conditions. This will be discussed on the basis of the experimental data reported in the previous paper[16].

Formation of the different phases and their interrelationship

Formation of the β-phase. The formation of the β-phase is a nucleation-controlled phenomenon, strongly influenced by the cooling rate. An increase of the scanning rate results in a shift of the crystallization temperature, T_m^β, to lower values. These experimental observations are in agreement with the general principles of polymer crystallization.

Crystallization into the β-phase can take place over the whole concentration range under well determined experimental conditions: (i) with the low molecular weight sample at intermediate and high polymer concentration ($\varphi_2 > 0.40$) and relatively low scanning rates; (ii) with the high molecular weight sample during a cooling experiment in the d.s.c. at intermediate and high polymer concentration ($\varphi_2 > 0.40$) at moderate scanning rates, and at low polymer concentration ($\varphi_2 < 0.40$) by isothermal annealing at temperatures higher than 70°C.

Only part of the polymer is transformed into the β-phase at the intermediate concentrations ($0.40 < \varphi_2 < 0.75$) during a dynamic experiment. This exothermic crystallization is stopped at around 148°C when $\varphi_2 = 0.63$ and at a scanning rate of $-5°\mathrm{C\,min^{-1}}$ (*Figure 3A*). The contribution of the β-phase to the total crystallinity decreases with increasing cooling rate. This temperature limit for the crystallization of the β-phase seems to be influenced by the overall polymer concentration. It is shifted to around 75°C when the concentration is greatly reduced. This concentration dependence of the temperature limit is reported in *Figures 1* and *4* and is based on observations with the high molecular weight sample. This can be done as the molecular weight does not seem to influence the formation and melting of the δ-phase. It then becomes clear, from extrapolation of the crystallization line to lower polymer concentration, that formation of the β-phase cannot take place below a polymer concentration of 0.55 and 0.29 for the low and high molecular weight samples, respectively.

The polymer crystallizes almost completely in this β-phase at high polymer concentrations ($\varphi_2 > 0.75$) when the solutions are cooled at moderate scanning rates. The degree of crystallinity, calculated on the basis of the amount of polymer in solution, is constant and equal to the value obtained in the absence of solvent.

The β-phase is also formed when crystallization is performed by cooling the melt or by heating a quenched, amorphous solvent-free sample.

The concentration dependence of the melting point of this β-phase is characteristic of the behaviour of a crystallized polymer in a rather good solvent.

Formation of the δ-phase. Formation of the δ-phase takes place at low temperature and necessitates a high degree of undercooling (up to 80°C) at the scanning rates used.

Complete transformation into this phase takes place at low polymer concentrations ($\varphi_2 < 0.50$) during a cooling experiment. Its melting enthalpy, calculated on the basis of the amount of polymer in solution, is almost constant except for the very dilute solutions.

In the intermediate concentration range ($0.50 < \varphi_2 < 0.75$) a competition between the formation of the β- and the δ-phase takes place. The degree of transformation into the δ-phase decreases with increasing polymer concentration at constant cooling rate and with decreasing cooling rate at constant polymer concentration. Quenching is necessary to prevent the formation of the β-phase and heating of the quenched solutions results in the formation of the δ-phase.

The structure formation mechanism does not fit the accepted principles of polymer crystallization, and a different mechanism can be proposed, similar to that already proposed for the system sPS–*trans*-decalin[16]. It is based on the experimental evidence reported for syndiotactic poly(methyl methacrylate) in *o*-xylene[24] and isotactic polystyrene in *cis*-decalin[25]. The first step consists of an intramolecular transition of the polymer chain in solution from a random coil to a segmented regular helical chain. An intermolecular association of regular segments, finally leading to gel formation, represents the second step. Microcalorimetric observations seem to provide some evidence for this two-step mechanism. There seems to be an upper temperature limit for this change in molecular conformation and this corresponds to the lower limit for the formation of the β-phase. This temperature limit increases with increasing polymer concentration.

The following mechanism for the formation of the different phases can then be proposed. Crystallization at high temperature takes place in a two-component polymer–solvent system. Once the solution is cooled below the temperature limit, a transformation from a coil to a helical conformation sets in and completely stops the crystallization into the β-phase. This transition is governed by an equilibrium constant. Further cooling shifts the equilibrium to the helical side and will increase the helical content of the solution. Once an appreciable amount of these regular structures is formed, intermolecular association can take place at the scanning rate used. The introduction of the equilibrium phenomenon between the formation of the β-phase and the δ-phase has to be considered as the most important factor responsible for the rather large degree of undercooling for the formation of the δ-phase in a dynamic experiment.

The solvent molecules play an important role in the formation of the regular helices and in the final crystalline structure. The δ-phase cannot be formed in the absence of solvent and therefore the formation of a compound between the polymer and the solvent is proposed. The exact role of the solvent is not completely understood at present.

Formation of the γ-phase. This phase can only be formed when the solvent is eliminated from the δ-phase. It cannot be obtained by quenching the solvent-free polymer into the low temperature region. This brings the system into the glassy region where crystallization is excluded.

Phase transitions. The δ-phase transforms into the β-phase upon heating by a mechanism of melting and recrystallization. The net result depends on the concentration and the scanning rate. The rate of recrystallization is high at high polymer concentration and both phenomena occur simultaneously. Only an exotherm is registered, resulting from the overlap of a melting endotherm of the δ-phase and an exotherm resulting from the recrystallization into the β-phase. In more dilute systems the recrystallization rate is reduced and the two phenomena occur separately. The melting of the δ-phase appears first and overlaps only partially with the recrystallization exotherm of the β-phase. Three phases coexist during this transformation: the δ-phase, the β-phase and the pure solvent, and this leads to an invariant situation. The δ-phase, a polymer–solvent compound, transforms into the β-phase and a solution by incongruent melting.

The δ-phase transforms into the γ-phase by evaporation of the solvent. This is an endothermic process. Further heating transforms the γ-phase into the β-phase at around 190–200°C. This is recorded as an exothermic process.

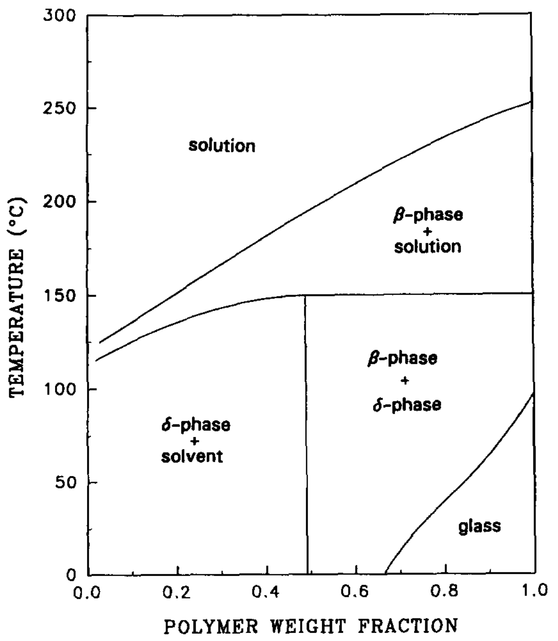

Figure 17 Schematic representation of the equilibrium phase diagram sPS–*o*-xylene, including the concentration dependence of the glass transition

No transformation of the β-phase to the δ-phase or γ-phase can be realized by thermal treatment. Swelling of a crystalline film does not affect the conformation of the polymer.

An amorphous film transforms into the δ-phase by swelling and into the β-phase by thermal treatment.

Interpretation of the phase diagram

The phase diagrams represented in *Figures 1* and *2* can be interpreted in view of the previous comments. This tentative interpretation is based on the data reported in this paper and in a previous paper on the thermal behaviour of sPS in decalin[16], and on data reported in the literature[26,27] for other systems. A schematic representation is given in *Figure 17.*

At high temperature the system acts as a quasi-two-component system composed of a polydisperse polymer, sPS, and a solvent, *o*-xylene. The most stable β-phase can be formed with the high molecular weight sample. Crystallization can take place at every concentration at temperatures above the temperature limit at which a change in the molecular conformation takes place. A decrease in the molecular weight results in a lower melting temperature and consequently in a lower crystallization temperature. This brings the crystallization temperature below the temperature limit of conformational change at concentrations $\varphi_2 < 0.40$. The formation of the less stable δ-phase takes over because of the occurrence of this intramolecular transformation, which proceeds much faster than the nucleation-controlled crystallization of the β-phase.

The composition of the polymer–solvent compound that constitutes the δ-phase is arbitrarily fixed at a molar ratio of styrene/*o*-xylene = 1. The solvent coexists with this compound at higher solvent contents and the melting line represents the transformation into the solution. At lower solvent contents this compound should be in equilibrium with the β-phase. This equilibrium, however, cannot be established as elimination of the solvent brings the polymer into the glassy phase. Melting results in transformation to the β-phase and a three-phase equilibrium is established, resulting in a constant melting point. This corresponds to an incongruent melting. Heating to higher temperatures results in melting of the β-phase.

ACKNOWLEDGEMENTS

The authors thank Dow Chemical Co., MI, USA, and Idemitsu Kosan Co., Japan, for supplying the polymer samples. The authors are indebted to the IWONL and DSM, the Netherlands, for a fellowship to F. D. The general financial support of the National Fund for Scientific Research and the Ministry of Scientific Programs through IUAP-16 is gratefully acknowledged. The authors also thank Professor R. Koningsveld for his interest and constructive advice.

REFERENCES

1 Ishihara, N., Seimiya, T., Kuramoto, M. and Uoi, M. *Macromolecules* 1986, **19**, 2464
2 Immirzi, A., de Candia, F., Iannelli, P. and Zambelli, A. *Makromol. Chem., Rapid Commun.* 1988, **9**, 761
3 Chatani, Y., Fujii, Y., Shimane, Y. and Ijitsu, T. *Polym. Prepr. Jpn* 1988, **37**, E428
4 Grassi, A., Longo, P. and Guerra, G. *Makromol. Chem., Rapid Commun.* 1989, **10**, 687
5 Kobayashi, M., Nakaoki, T. and Ishihara, N. *Macromolecules* 1989, **22**, 4377
6 Guerra, G., Vitagliano, V., De Rosa, C., Petraccone, V. and Corradini, P. *Macromolecules* 1990, **23**, 1539
7 Guerra, G., Musto, P., Karasz, F. and MacKnight, W. *Makromol. Chem.* 1990, **191**, 2111
8 Capitani, D., Segre, A., Grassi, A. and Sykora, S. *Macromolecules* 1991, **24**, 623
9 De Rosa, C., Guerra, G., Petraccone, V. and Corradini, P. *Polym. J.* 1991, **23**, 1435
10 Rapacciuolo, M., De Rosa, C., Guerra, G., Mensitieri, G., Apicella, A. and Del Nobile, M. *J. Mater. Sci. Lett.* 1991, **10**, 1084
11 Wang, Y., Savage, J., Young, D. and Hsu, S. L. *Macromolecules* 1992, **25**, 3659
12 Capitani, D., De Rosa, C., Ferrando, A., Grassi, A. and Segre, A. *Macromolecules* 1992, **25**, 3874
13 Chatani, Y., Shimane, Y., Inoue, Y., Inagaki, T., Ishioka, T., Ijitsu, T. and Yukinari, T. *Polymer* 1992, **33**, 488
14 Sun, Z., Morgan, R. and Lewis, D. *Polymer* 1992, **33**, 660
15 De Rosa, C., Rapacciuolo, M., Guerra, G., Petraccone, V. and Corradini, P. *Polymer* 1992, **33**, 1423
16 Deberdt, F. and Berghmans, H. *Polymer* 1993, **34**, 2193
17 Nyquist, R. *Appl. Spectrosc.* 1988, **43**, 440
18 Reynolds, M., Savage, J. and Hsu, S. L. *Macromolecules* 1989, **22**, 2867
19 Kobayashi, M., Nakaoki, T. and Ishihara, N. *Macromolecules* 1990, **23**, 78
20 Reynolds, M. and Hsu, S. L. *Macromolecules* 1990, **23**, 3463
21 Vittoria, V. *Polym. Commun.* 1990, **31**, 263
22 Filho, A. and Vittoria, V. *Makromol. Chem., Rapid Commun.* 1990, **11**, 199
23 Reynolds, M., Stidham, H. and Hsu, S. L. *Macromolecules* 1991, **24**, 3662
24 Thijs, S. Doctoral thesis, Katholieke Universiteit, Leuven, 1991
25 Jacobs, A. Doctoral thesis, Katholieke Universiteit, Leuven, 1991
26 Guenet, J. M. and McKenna, G. *Macromolecules* 1988, **21**, 1752
27 Point, J. and Damman, P. *Macromolecules* 1992, **25**, 1184